September 20-23, 2011
City of Cuernavaca México
XI International
Hydrogen Congress
an event of The Mexican Hydrogen Society
Cuernavaca...
The Endless Spring

# COMPARISON OF VARIABLE RESISTANCE AND LINEAR SWEEP VOLTAMMETRY METHODS FOR CHARACTERIZING A MEDIATOR-LESS SINGLE CHAMBER MICROBIAL FUEL CELL LOADED WITH SULFATE REDUCING BIOCATALYSTS

K. Sathish Kumar[1], Omar Solorza-Feria[2,1], Gerardo Vazquez-Huerta[2],
Héctor M. Poggi-Varaldo[3,1*]

[1]Doctoral Program of Nanoscience and Nanotechnology, Centro de Investigación y de Estudios Avanzados del IPN, Apdo. Postal 14-740, 07360 Mexico D.F.

[2]Depto. Química, Centro de Investigación y de Estudios Avanzados del IPN, Apdo. Postal 14-740, 07360 México D.F.

[3]Depto. Biotecnología y Bioingeniería, Centro de Investigación y de Estudios Avanzados del IPN, Apdo. Postal 14-740, 07360 México D.F.

[*] contact email: hectorpoggi2001@gmail.com

## ABSTRACT

A single-chamber microbial fuel cell (SCMFC) with a carbon supported Pt-cathode for the oxygen reduction reaction (ORR), and a sulfate reducing bacterial consortium as biocatalyst in the anodic chamber was characterized by polarization of variable resistance (VR) and linear sweep voltammetry (LSV). From VR a maximum power density of 16 mW $m^{-2}$ ± 4.06 was attained at a current density of 75.5 mA $m^{-2}$ ± 13.55 and voltage of 0.21 V ± 0.105. The LSV method gave a maximum power density of 20.2 mW $m^{-2}$ ± 80.09 at current density of 202 mA $m^{-2}$ ± 27.24 at the potential of 0.10V ± 0.17. Internal resistance values were 764 Ω and 884 Ω, determined by VR method and electrochemical impedance spectroscopy, respectively. Reasonable agreement values of electrochemical characteristics of the SCMFC between both methods were found, although the maximum power densities determined by LSV were 20% higher than that obtained by resistance methods.

**Key words:** Oxygen reduction reaction, polarization, resistance, sulfate-reducing bacteria.

## 1. INTRODUCTION

A microbial fuel cell (MFC) is a promising renewable energy source; in the anodic chamber the microorganisms anoxically oxidize the organic compounds and release electrons and protons. Electrons are channeled to the anode that acts as external electron sink. Protons are released in organic matter oxidation, and they migrated through proton exchange membrane to the cathode. There, the transported protons react with the oxygen producing water in the presence of carbon-supported Pt nanoparticles [1-2]. Collected electrons are directed to an external circuit where there is a resistor or a device to be powered, in this way direct current is produced.

There are a variety of factors that can affect the overall performance of a MFC [3-11]. Biocatalyst used is one of them. A few works with MFC using sulphate reducing bacteria have been reported [12, 13]. Recently, our Group has observed a 13 fold substantial improvement in volumetric power ($P_v$) of a MFC using sulphate reducing bacteria, compared to methanogenic and aerobic inocula [9].

Estimates of the maximum power that can be produced in a MFC can be a function of the technique used to obtain the polarization curve [14,15]. In the variable resistance (VR) method the circuit resistance is varied at fixed time intervals, ranging from 10s to 24h. An alternative approach is sweeping the potential at different scan rates using a technique called linear sweep voltammetry (LSV)[16].

There have been very few studies comparing the above metioned techniques [15], but in one study it was found that power production with scan rates higher than 0.1 mV/s produced higher power densities than those with the VR method. A common problem often encountered when evaluating polarization curve is “power overshoot” [15, 18-20]. Power overshoot refers to the response of the system at high current densities (past the maximum power) in a power density curve where the cell voltage and current drop very quickly resulting in a doubling back of the power density curve, producing lower power than previously measured for the lower current densities. One hypothesis on the cause of this power overshoot is that as the current resistance is decreased the bacteria on the anode are unable to produce sufficient current at lower voltages

[19]. However, it does not seem to be a correlation in the literature between the magnitude of current density and power curve shape [16]. The aim of our research was to compare the two methods of polarization (LSV and VR) in the characterization of a MFC loaded with a sulphate reducing inoculum.

## 2. MATERIALS AND METHODS

### 2.1. Construction of single chamber vertical MFC

MFC consisted of a vertical cylinder built in Plexiglass 9 cm long and 5.6 cm internal diameter (Fig. 1).

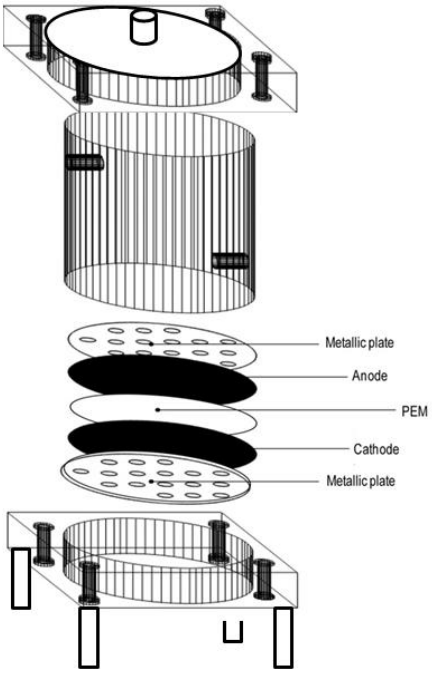


**Figure 1.** Schematic diagram of the vertical single chamber MFC

An assemblage of anode-proton exchange membrane-cathode was fitted at the bottom of the cell. For brevity, this 'sandwich' arrangement was abbreviated as AMC (for Anode-proton exchange Membrane- Cathode.)

The AMC consisted of (from inside to outside) a circular, perforated stainless steel plate 1 mm thickness covered below with a Toray flexible carbon-cloth sheet, a proton exchange membrane (Nafion 117), a flexible carbon-cloth containing 0.5mg $cm^{-2}$ Pt catalyst (10wt%/C-ETEK) as cathode, and a perforated plate of stainless steel 1 mm thickness. The area of the circular electrodes was 0.0023 $m^2$.

2.2. Model extracts (fuel) and biocatalysts.

The cells were loaded with 7 mL from a model extract similar to that produced in the anaerobic fermentation of solid wastes and 193 mL of a sulphate-reducing inoculums (liquor from a suspended-growth sulphate reducing bioreactor.) The model extract consisted of a mixture of the following substance (in g/L): acetone, ethanol, acetic, propionic, and butyric acids (4 each), mineral salts such as $NaHCO_3$ and $Na_2CO_3$ (3 each) and $K_2HPO_4$ and $NH_4Cl$ (0.6 each). Organic matter concentration of model extract was ca. 25 gCOD/L, whereas the initial organic matter concentration in the cell content was 1120 mg COD/L.

2.3 Evaluation of single chamber vertical MFC efficiency

*2.3.1 Variable resistance method*

The MFC was loaded with substrate and inoculum as described in section 2.2. MFC was batch-operated for 7 h at 35ºC. First, the MFC was operated at open circuit for 1 h. Afterwards; the external resistance $R_{ext}$ was varied from 10Ω to 1MΩ than 1MΩ to 10Ω. After this, the cell was set to open circuit condition for 1 h in order to check the adequacy of the procedure (values of initial and final open circuit voltages should be close). The voltage was measured and recorded with a Multimeter ESCORT 3146A. The current intensity (I) was calculated by Ohm`s law:

$$I=E/R \quad (1)$$

The delivered power was obtained as the product of the current intensity times the voltage, that is:

$P=I \times E$ (2)

*2.3.2 Linear sweep voltammetry*

Liner sweep voltammetry (LSV), was run at the recommended scan rate of 1mV $s^{-1}$ starting from the measured open circuit potential [21] using a 273A Potentiostat/Galvanostat from EG&G Princeton Applied Research.

*2.3.3 Determination of internal resistance*

The internal resistance of cells was determined using the polarization curve method, by varying the external resistance ($R_{ext}$) and monitoring both the voltage and current intensity, according to procedures suggested elsewhere [20, 22]. Electrochemical impedance spectroscopy (EIS) measurements were performed at the open circuit potential ($V_{OCP}$) and two applied cell voltages: $V_{100}$ and $V_0$. The frequency range was 100 kHz-1mHz, the amplitude of the signal perturbation was 10mV.

## 3. RESULTS AND DISCUSSION

The single chamber MFC was operated at open circuit voltage for 1 h; a maximum voltage of 0.712 V was attained. Afterwards, the $R_{ext}$ was varied from 10Ω to 1MΩ and backwards. After this, the cell was again kept at OCP conditions for 1 h to check that the maximum voltage was attained again (Fig. 2), that is, 0.71 V. This feature validated the application of the VR to our cell. With the VR method, the system achieved the maximum power density of 16 mW/$m^2$ ± 4.06 at current density of 75.5 mA/$m^2$ ± 13.55 and Voltage of 0.21 V ± 0.105 (Fig. 3). Reasonable agreement values of electrochemical characteristics of the SCMFC between both methods were found, although the maximum power densities determined by LSV was 20% higher than that obtained using either of the resistance methods. Our results were in agreement with previously reports in the literature [15,16].

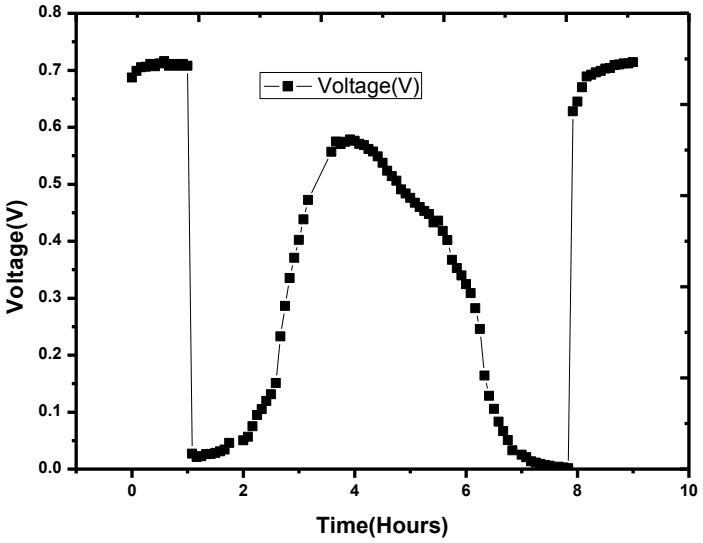


**Figure 2.** Voltage vs. time curve behavior of single chamber mediator-less MFC

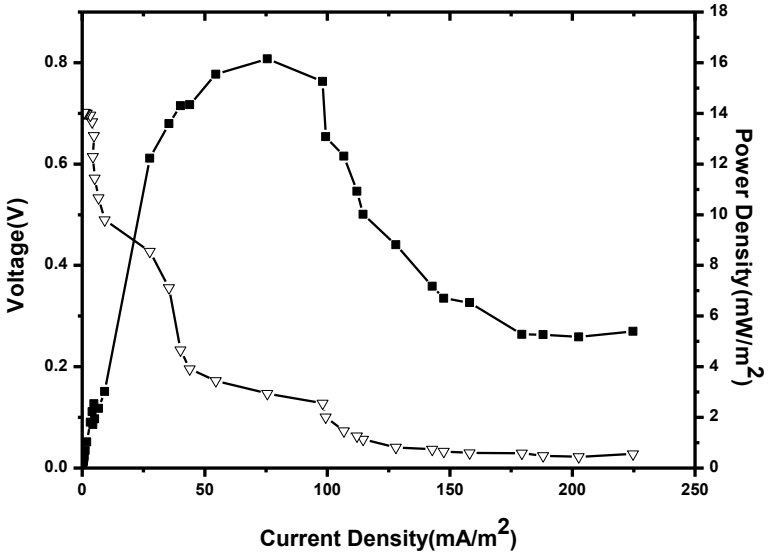


**Figure 3.** Polarization behavior of single chamber mediator-less MFC-VR method.

Keys: black squares, power density; hollow triangles, voltages

One possible reason for observing a higher power density with the LSV method is that with this technique the long times between switching circuit loads during a fed-batch cycle for biological systems are avoided or eliminated [17].

The internal resistance ($R_{int}$) is one of the main characteristics of a MFC, because high values tend to result in low power output of the cell. On the other hand, according to Jacobi's theorem of maximum power delivered by an electromotive force, a MFC fitted with an external resistance equal to its internal resistance will give its maximum power output [23]. The polarization curve is shown in Fig. 3. The regression line based on Fig. 3 data was

$E = -764.9*I + 0.7553; \quad R^2 = 0.9986$ (3)

Where E is the voltage and I is the current intensity

The internal resistance of the cell was 765 Ω determined using the polarization curve [2, 8, 9, 20-21] (Fig.4).

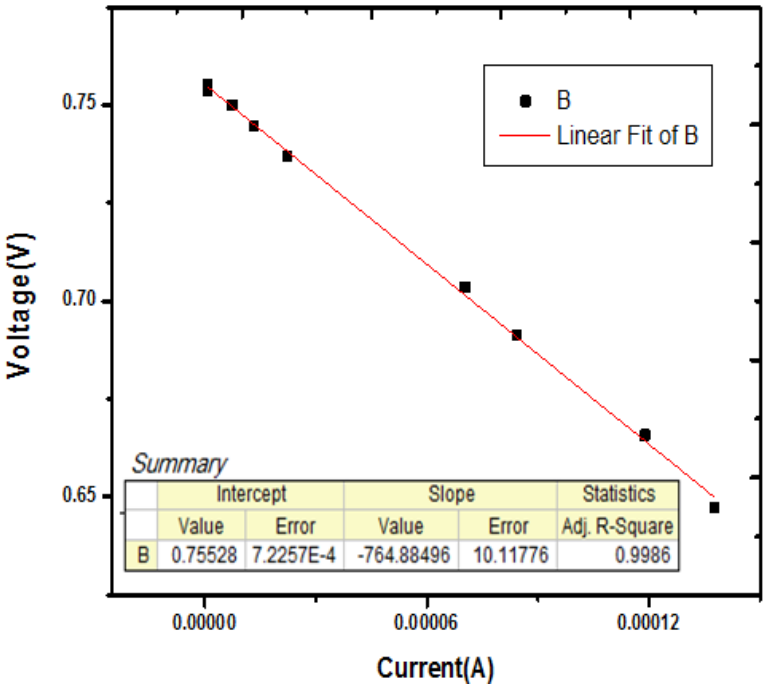


**Figure 4.** $R_{int}$ of single chamber mediator-less MFC-VR method

The LSV method yielded a maximum power density of 20.2 mW/m$^2$ ± 80.09 at the current density of 200 mA/m$^2$ ± 27.24 and potential of 0.100 V ± 0.17 (Fig. 5).

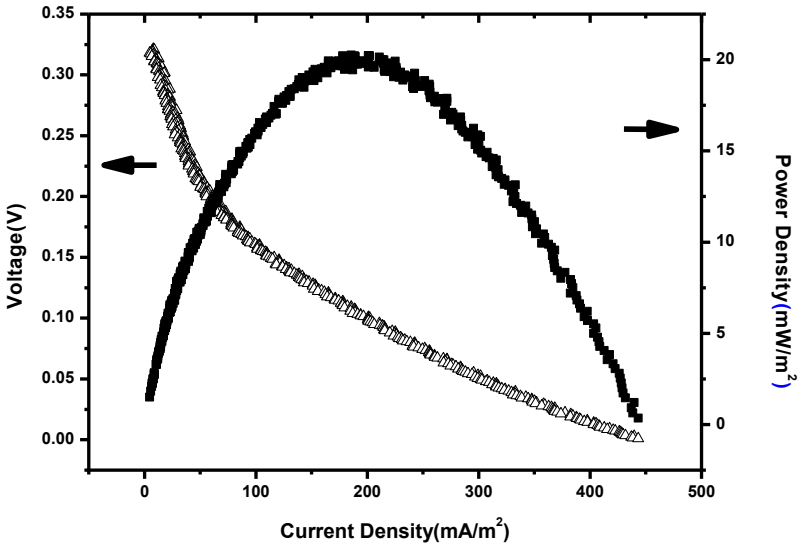


**Figure 5.** Polarization behavior of single chamber MFC-LSV method.

Fig. 6 shows the EIS spectra of the SCMFC at three different applied cell voltages. Inset in this figure shows the electric circuit that fits the impedance spectra. The internal resistance of the MFC is defined as $R_{int}$=$R_{anode}$ ($R_a$)+ $R_{cathode}$($R_c$)+$R_{membrane}$ ($R_m$). $QPE_c$ and $QPE_a$ are related to the double layer capacitance of the cathode and anode respectively. Applied cell voltages were close to the short circuit ($V_0$), 100 mV potential ($V_{100}$) and open circuit potential ($V_{OCP}$).

The parameters of the electrical circuits that best fitted the impedance spectra are listed in Table 1. At OCP the MFC showed a $R_{int}$ of 884 Ω. At the applied potential of 100mV ($V_{100}$) and 0 mV ($V_0$) the values of $R_{int}$ were 372 and 194Ω, respectively. In the case of anode and cathodes their resistances were drastically reduced, probably due to short circuit potential of the system. Yet, the membrane contribution to resistance was kept approximately constant; it can be inferred that external potential did not affect the membrane resistance. In all cases $R_{int}$ decreased with the

applied cell voltage and increasing the current flow, in agreement with results reported elsewhere [22].

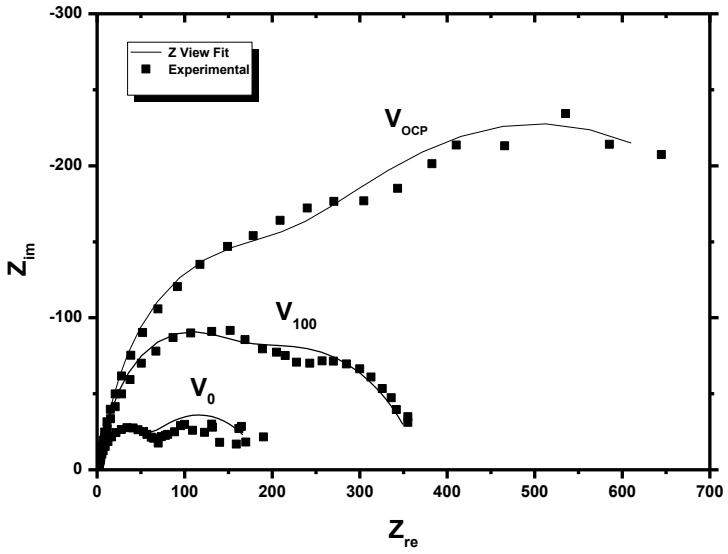


**Figure 6.** $V_{OCP}$, $V_{100}$, $V_0$, at three different applied cell voltages to measure $R_{int}$-by the EIS method

**Table 1.** Parameter values obtained by $R_{int}$-EIS methods at three different applied cell voltages ($V_{OCP}$, $V_{100}$, $V_0$)

| **Applied Cell Voltage(mV)** | **$R_{anode}$(Ω)** | **$R_{cathode}$(Ω)** | **$R_{membrane}$(Ω)** | **$R_{int}$ [a] (Ω)** |
|---|---|---|---|---|
| **OCP [b] (mV)** | 736±4.2 | 148±2.1 | 1.331±0.001 | 884±2.1 |
| **$V_{100}$ [c] (mV)** | 255±2.8 | 115±3.5 | 1.326±0.001 | 372±7.1 |
| **$V_0$ [d] (mV)** | 151±2.8 | 41±2.1 | 1.299±0.006 | 194±5.7 |

Notes: [a] $R_{int}=R_{anode}+R_{cathode}+R_{membrane}$; [b] potential at open circuit; [c] potential at 100mV; [d] potential at 0mV

In order to monitor the internal resistance of the system with respect to time and possibly with respect to bacterial growth behaviour, several EIS spectra were acquired at different times under OCP conditions (Fig.7).

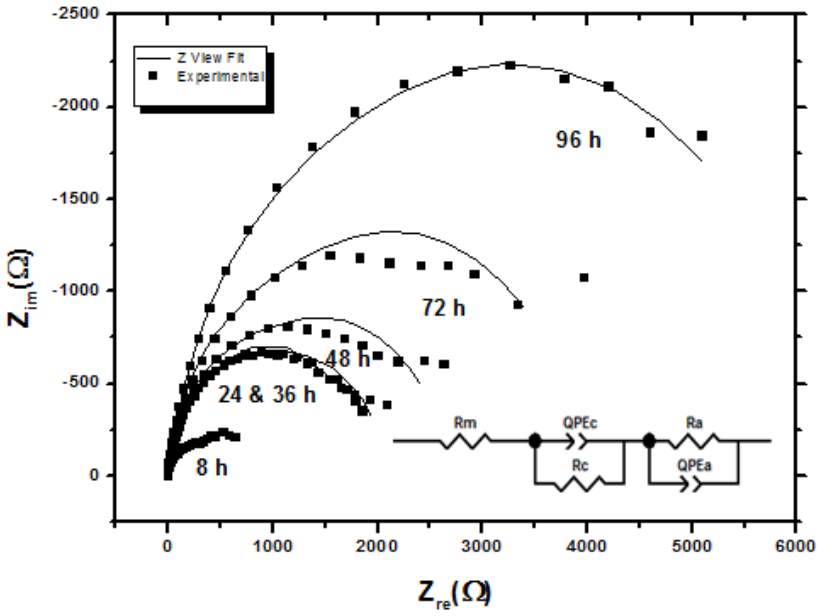


**Figure 7.** Different time intervals' to measure $R_{int}$-EIS method at Open circuit potential condions.

Fitted parameter values at different time are listed in Table 2. In general, $R_{int}$ increased with time. It seems that bacterial growth attained the maximum at 8h which was reflected in the maximum steady state potential of the MFC at that time. Afterwards, the potential tends to decrease, due to the declining phase of bacterial growth. On that time the internal resistance of MFC also increases from 2100Ω on 24 hours to 6361Ω on 96 hours. This behaviour could be associated with loss of activity of the bacteria and leads to the decline phase. The contribution of the anodic resistance alone accounted for 70 to 80% of the total internal resistance value (Table 2).

**Table 2.** Values of $R_{int}$ obtained by EIS method at different times at OCP conditions.

| Time (hours) | $R_{anode}(\Omega)$ | $R_{cathode}(\Omega)$ | $R_{membrane}(\Omega)$ | $R_{int}{}^{a}(\Omega)$ |
|---|---|---|---|---|
| **8** | 736±4.24 | 148±1.41 | 1.331±0.001 | 884±5.66 |
| **24** | 1604±2.83 | 493±2.12 | 1.342±0.002 | 2100±6.36 |
| **36** | 1657±1.41 | 483±1.41 | 1.347±0.001 | 2147±1.41 |
| **48** | 2199±0.71 | 533±1.41 | 1.351±0.045 | 2740±2.82 |
| **72** | 3421±2.12 | 616±4.24 | 1.358±0.002 | 4048±9.19 |
| **96** | 5527±1.41 | 822±1.41 | 1.409±0.006 | 6361±10.61 |

Notes: $^{a}R_{int}=R_{anode}+R_{cathode}+R_{membrane}$

Fig 8. shows the $R_{int}$ with respect to the time, the behavior of the curve fits an exponential model. This suggests an association with bacterial growth by exponential relationship Eq. 4. In 24 and 36 h $R_{int}$ maintained steadily; afterwards $R_{int}$ increased, probably due to decline phase of the bacterial growth. The exponential curve that fitted our data was

$$R_{int}(t) = a * \exp(b * t); \quad R^2 = 0.9829 \qquad (4)$$

where a is the initial resistance equal to 1122 Ω; b is an exponent equal to 0.01807 (1/h)

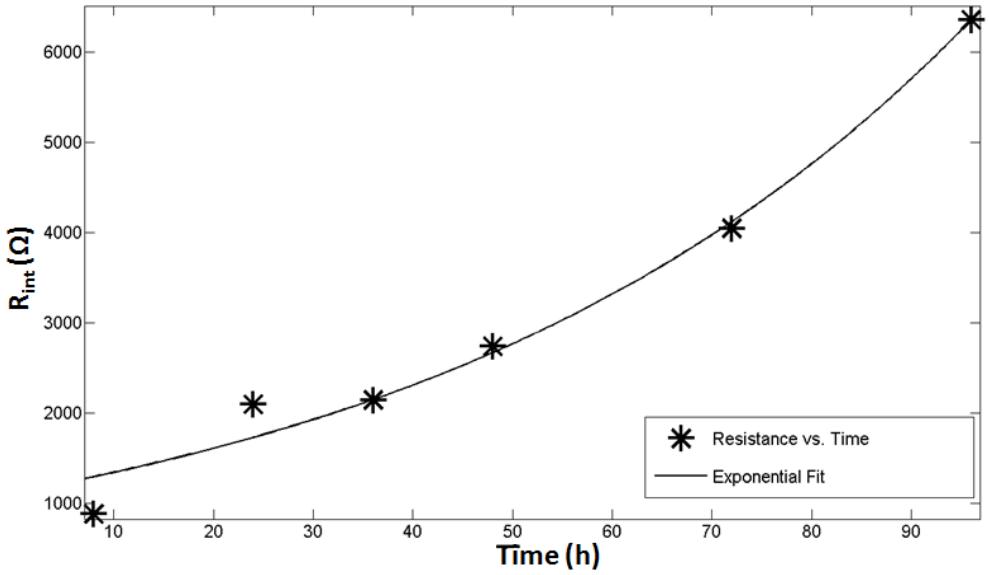


**Figure 8.** Exponential curve fit of Time vs $R_{int}$

It could be assumed that the kinetics of the anode is slower than that of the cathode [23]. Therefore, we assigned the highest value of the fit to $R_a$ . The cathode resistance $R_c$ was the second resistance of the circuit in importance. On the other hand, $R_m$ was the smallest.

## 4. CONCLUSIONS

A vertical single-chamber microbial fuel cell was constructed, loaded with a sulfate reducing bacterial consortium, and characterized by using variable resistance method (VR) and linear sweep voltammetry (LSV). The maximum power density obtained by VR was 16 mW $m^{-2}$ ± 4.06 at the current density of 75.5 mA $m^{-2}$ ± 13.55 and a voltage of 0.21V ± 0.105. On the other hand, the LSV method gave a maximum power density of 20.2 mW $m^{-2}$ ± 80.09 at current density of 202 mA $m^{-2}$ ± 27.24 at the potential of 0.10V ± 0.17. The internal resistance of the SCMFC was evaluated by using VR method and electrochemical impedance spectroscopy obtaining 764 Ω and 884 Ω respectively, a reasonable agreement between both methods was found. A study of Rint versus time of cell operation in the range 8 to 96 h showed a significant increase of Rint the

the range of 8 to 96 h, possibly related to the pattern of growth of the inoculum (growth, stationary, and declining phases).

## 5. ACKNOWLEDGEMENTS

The insightful comments of the Editor of the Scientific Committee as well as anonymous Reviewers of the Mexican Society for Hydrogen are gratefully acknowledged. One of the authors (KS-K) thanks SEP and CINVESTAV for scholarship support. Excellent technical help of personnel of Fuel Cell Group (Dept. of Chemistry) and Environmental Biotechnology and Renewable Energies Group (Dept. of Biotechnology and Bioengineering), both of CINVESTAV del IPN, is appreciated.

## 6. REFERENCES

[1] B. E. Logan, B. Hamelers, R. Rozendal, U. Schröder, J. Keller, S. Freguia, P. Aelterman, W. Verstraete, K. Rabaey, *Environmental Science & Technology*, **40**, 5181 (2006).

[2] Poggi-Varaldo HM, Vazquez-Larios AL, Solorza-Feria O. Capítulo 7. Celdas de combustible microbianas. In: Rodríguez-Varela FJ, Solorza-Feria O, Hernández-Pacheco E (Editores). *Celdas de combustible.* 2010. Ed. Books Livres, Montréal, Canadá. pp 123-161. ISBN 978-0-9809915-2-9.

[3] Vázquez-Larios AL, Solorza-Feria O, Poggi-Varaldo HM. Capítulo 9. Efecto del tipo de inóculo sobre el desempeño de una celda de combustible microbiana de nuevo diseño. In: Ríos-Leal E, Solorza-Feria O, Poggi-Varaldo HM (Editores). Energías Renovables Biológicas – Hidrógeno - Pilas de combustible- II. 2010. ISBN 978-607-00-3608-8. CINVESTAV del IPN e ICYTDF. México D.F., México. pp. 133-146. Book in CD-ROM.

[4] Vázquez-Larios AL, Ríos-Leal E, Solorza-Feria O, Poggi-Varaldo HM. Capítulo 10. Influencia de la temperatura sobre las características y desempeño de celdas de combustible microbiana. In: Ríos-Leal E, Solorza-Feria O, Poggi-Varaldo HM (Editores). Energías Renovables Biológicas – Hidrógeno - Pilas de combustible- II. 2010. ISBN 978-607-00-3608-8. CINVESTAV del IPN e ICYTDF. México D.F., México. pp. 147-158. Book in CD-ROM.

[5] Vázquez-Larios AL, Solorza-Feria O, Vazquez-Huerta G, Poggi-Varaldo HM. Capítulo 11. Determinación de la resistencia interna de una celda de combustible microbiana de nuevo tipo con dos métodos de caracterización. In: Ríos-Leal E, Solorza-Feria O, Poggi-Varaldo HM (Editores). Energías Renovables Biológicas – Hidrógeno - Pilas de combustible- II. 2010. ISBN 978-607-00-3608-8. CINVESTAV del IPN e ICYTDF. México D.F., México. pp. 159-167. Book in CD-ROM.

[6] Ortega-Martínez AC, Vázquez-Larios AL, Hernández-Flores G, Juárez-López K, Galíndez-Mayer J, Rinderknecht-Seijas N, Ponce-Noyola MT, Solorza-Feria O, Poggi-Varaldo HM. Capítulo 12. Procedimientos de enriquecimiento de bacterias electroquímicamente activas en celda de combustible microbiana y ventajas del uso de biocátodos . In: Ríos-Leal E, Solorza-Feria O, Poggi-Varaldo HM (Editores). Energías Renovables Biológicas – Hidrógeno - Pilas de combustible- II. 2010. ISBN 978-607-00-3608-8. CINVESTAV del IPN e ICYTDF. México D.F., México. pp. 168-189. Book in CD-ROM.

[7] Ortega-Martínez AC, Juárez-López K, Galíndez-Mayer J, Rinderknecht-Seijas N, Ponce-Noyola MT, Solorza-Feria O, Poggi-Varaldo HM. Capítulo 13. Minimización de resistencia interna en una celda de combustible microbiana de nueva arquitectura. In: Ríos-Leal E, Solorza-Feria O, Poggi-Varaldo HM (Editores). Energías Renovables Biológicas – Hidrógeno - Pilas de combustible- II. 2010. ISBN 978-607-00-3608-8. CINVESTAV del IPN e ICYTDF. México D.F., México. pp. 190-205. Book in CD-ROM.

[8] A.L. Vazquez-Larios, O. Solorza-Feria, G. Vazquez-Huerta, E. Rios-Leal, N. Rinderknecht-Seijas[3] and H.M. Poggi-Varaldo, *JNMES*, **14(2)**, 99-105 (2011).

[9] A. L. Vázquez-Larios, O. Solorza-Feria, G. Vázquez-Huerta, F. Esparza-García, N. Rinderknecht-Seijas, H. M. Poggi-Varaldo, *International Journal of Hydrogen Energy*, **36**, 6199 (2011).

[10] H. Liu, S. Cheng, B. E. Logan, *Environmental Science & Technology*, **39**, 5488 (2005).

[11] B. Min, S. Cheng, B. E. Logan, *Water Research*, **39**, 1675 (2005).

[12] Habermann, W., Pommer, E.-H, *Appl. Microbiol. Biotechnol.* **35**, 128 (1991).

[13] Cooney, M.J., Roschi, E., Marison, I.W., Comninellis, Ch., Stockar, U, *Enzyme Microb. Technol.* **18**, 358 (1996).

[14] Y. Zuo, S. Cheng, D. Call, B. E. Logan, *Environmental Science & Technology*, *41*, 3347 (2007).

[15] J. Menicucci, H. Beyenal, E. Marsili, Veluchamy, G. Demir, Z. Lewandowski, *Environmental Science & Technology*, **40**, 1062 (2005).

[16] S. B. Velasquez-Orta, T. P. Curtis, B. E. Logan, *Biotechnology and Bioengineering*, **103**, 1068 (2009).

[17] V. J. Watson, B. E. Logan, *Electrochemistry Communications*, **13**, 54 (2011).

[18] P. Aelterman, K. Rabaey, H. T. Pham, N. Boon, W. Verstraete, *Environmental Science & Technology*, **40**, 3388 (2006).

[19] J. R. Kim, G. C. Premier, F. R. Hawkes, J. Rodríguez, R. M. Dinsdale, A. J. Guwy, *Bioresource Technology*, **101**, 1190 (2010).

[20] I. Ieropoulos, J. Winfield, J. Greenman, *Bioresource Technology*, **101**, 3520 (2010).

[21] B. E. Logan, B. Hamelers, R. Rozendal, U. Schröder, J. Keller, S. Freguia, P. Aelterman, W. Verstraete, K. Rabaey, *Environmental Science & Technology*, **40**, 5181 (2006).

[22] P. Clauwaert, K. Rabaey, P. Aelterman, L. De Schamphelaire, T. H. Pham, P. Boeckx, N. Boon, W. Verstraete, *Environmental Science & Technology*, **41**, 3354 (2007).

[23] Halliday D, Resnick R, Walker J. In: Fundamentals of Physics. 7th ed.. New York: John Wiley & Sons Co., ISBN 978-0-471-21643-8; 2004.

[24] A. K. Manohar, F. Mansfeld, *Electrochimica Acta*, **54**, 1664 (2009).

[25] Q. Wen, Y. Wu, L.-x. Zhao, Q. Sun, F.-y. Kong, *Journal of Zhejiang University - Science B*, **11**, 87 (2009).

**NOTATION**

| | |
|---|---|
| AMC | assemblage (sandwiched) anode-membrane-cathode |
| EIS | electrochemical impedance spectroscopy |
| MS | manuscript |
| LSV | linear sweep voltammetry |
| MFC | microbial fuel cell |
| OCP | open circuit potential |
| ORR | oxygen reduction reactions |
| $P_v$ | volumetric power |

| | |
|---|---|
| $QPE_a$ | double layer capacitance of the anode |
| $QPE_c$ | double layer capacitance of the cathode |
| $R_a$ | anodic resistance |
| $R_c$ | cathodic resistance |
| $R_{ext}$ | external resistance |
| $R_{int}$ | internal resistance |
| $R_m$ | membrane resistance |
| SCMFC | single chamber microbial fuel cell |
| VR | variation of resistance |